Contrib Mineral Petrol (1997) 129: 166–181

Bernard J. Wood · Jonathan D. Blundy

A predictive model for rare earth element partitioning between clinopyroxene and anhydrous silicate melt

Received: 8 November 1996 / Accepted: 28 May 1997

Abstract We present a quantitative model to describe the partitioning of rare earth elements (REE) and Y between clinopyroxene and anhydrous silicate melt as a function of pressure (P), temperature (T) and bulk composition (X). The model is based on the Brice (1975) equation, which relates the partition coefficient of element i (D_i) to that of element o (D_o) where the latter has the same ionic radius r_o as the crystallographic site of interest, in this case the clinopyroxene M2 site:

$$D_i = D_o \exp\left(\frac{-4\pi E_{M2} N_A \left(\frac{r_o}{2}(r_i - r_o)^2 + \frac{1}{3}(r_i - r_o)^3\right)}{RT}\right)$$

N_A is Avogadro's number, E_{M2} is the Young's Modulus of the site, R is the gas constant and T is in K. Values of E_{M2} obtained by fitting the Brice equation to experimental REE partition coefficient patterns are in good agreement with those obtained from the well-known correlation between bulk modulus, metal-oxygen distance and cation charge. Using this relationship to constrain E_{M2} for 3+ cations and then fitting the Brice equation to those experimental data where 3 or more REE partition coefficients had been simultaneously measured we obtained 82 values of D_o and r_o. The latter was found to be a simple and crystallochemically reasonable function of clinopyroxene composition. We show that for any clinopyroxene-melt pair if D for one middle REE (e.g. Sm or Gd) is known then the Brice equation can be used to predict Ds for all the other REE, with uncertainties similar to those involved in the actual measurements. The model was generalised using thermodynamic descriptions of REE components in crystal and melt phases to estimate the free energy of fusion (ΔG_f) of the fictive REE components $REEMgAlSiO_6$ and $Na_{0.5}REE_{0.5}MgSi_2O_6$. For the melt we find that 6-oxygen melt components ($CaMgSi_2O_6$, $NaAlSi_2O_6$, $Mg_3Si_{1.5}O_6$ etc.) mix with constant activity coefficient over a wide range of natural compositions. Propagating ΔG_f into the Brice model we obtain an expression for D_o^{3+} in terms of the atomic fraction of Mg on the clinopyroxene M1 site, the *Mg*-number of the melt, P and T. The D for any REE can be calculated from D_o^{3+} using the Brice equation. Over 92% of D_{REE} (454 points) calculated in this way lie within a factor 0.63–1.59 of the experimental value. The approach can be extended to calculate D for any REE at a given P (≤ 6 GPa) and T (1200–2038 K) to within 0.60–1.66 times the true value given only the crystal and/or melt composition. The model has widespread applicability to geochemical modelling of all natural processes involving clinopyroxene, e.g. decompression mantle melting, enabling for the first time account to be taken of variations in partition coefficient in response to changing pressure, temperature and phase composition.

Introduction

Since the development of accurate methods of determining element concentration at the parts per million (ppm) level the trace element contents of igneous rocks have frequently been used to model their chemical evolution. These studies use estimated crystal-liquid partition coefficients together with solutions for the differential equations describing, for example, fractional crystallisation or fractional melting (Shaw 1970) to model evolution of the melt during precipitation or dissolution of the crystalline phases. Generally, because of lack of data, the crystal-liquid partition coefficients are assumed to be constant during differentiation, an assumption which is thermodynamically implausible and which contradicts observed variations in partition coefficients (Jones 1995). This is a fundamental limitation in the use of trace element partition coefficients in petrogenetic modelling of polythermal, polybaric processes.

B.J. Wood (✉) · J.D. Blundy
CETSEI, Department of Geology, University of Bristol, Bristol, BS8 1RJ, UK

Editorial responsibility: A. Hofman

Until the effects of pressure, temperature and composition on element partitioning are known, the results, independent of the type of fractionation process involved, are bound to be subject to large uncertainty. Our aim here is to develop a method of predicting variations in partition coefficients using thermodynamic principles in combination with a recently developed model which relates partitioning to ionic radius, lattice strain and elastic constants. Because of their petrogenetic importance we focus mainly on the partitioning of rare earth elements (REE) between clinopyroxene and melt. However the approach can be generalised to other elements and minerals.

Background

Consideration of crystal-liquid equilibrium from a thermodynamic standpoint indicates that partitioning should depend on pressure, temperature and bulk composition (e.g. Wood and Fraser 1976, pp. 199–200). Separating the different effects is difficult, however, because, for any given crystal-melt pair, temperature, pressure and composition are strongly correlated. This is illustrated by the partitioning of Sr and Ba between plagioclase feldspar and silicate melt. The partition coefficients are apparent functions of temperature and bulk composition and were fitted by Nielsen (1988) to an equation in reciprocal temperature after taking explicit account of bulk compositional effects in the melt using a 2-lattice model. Bulk compositional controls may, however be exercised by the silicate melts or by the plagioclase crystals or by both. Since the plagioclase and melt compositions are strongly correlated, it is difficult to determine their relative importance. Blundy and Wood (1991) argued the opposite case to that assumed by Nielsen (1988), namely that the bulk compositional effects of the crystals should dominate over those of the melt. The rationale is that the large cations, Ba and Sr, much more easily replace smaller Na and Ca in the relatively flexible melt structure than in the rigid crystal structure. The introduction of large Ba or Sr ions into a smaller lattice site generates elastic strain energy, the amount of which depends on the Young's modulus of the medium. Since the Young's modulus of a phase with no shear modulus, such as silicate melt, is zero, the strain energy must be dominated by the elastic properties of the crystals, which have Young's moduli in the range 100–300 GPa.

Blundy and Wood (1991) were able to demonstrate that crystal composition, rather than melt composition or temperature exerts the greatest control on Ba and Sr feldspar-liquid partition coefficients, which range from about 0.1 to 8.0 and 1.2 to 33 respectively in igneous systems, by considering the data of Lagache and Dujon (1987). The latter authors found, at constant temperature, a strong dependence of Sr partitioning between plagioclase and aqueous solutions on the anorthite content of the feldspar. Since the solutions they used were extremely dilute (1 Molal), the effects they observed must be almost entirely due to the compositional variations of the crystals. Blundy and Wood (1991) demonstrated that when the plagioclase/fluid partitioning results were recast on a molar rather than weight basis, the dependence of D_{Sr} on X_{An} is exactly the same as that observed in polythermal plagioclase-silicate melt experiments (Fig. 1). Therefore, solution or melt composition must play a subordinate role to that of the crystal, at least in the case of Sr and Ba partitioning between plagioclase and melt or fluid.

In order to quantify the effects of elastic strain energy on partition coefficients, Blundy and Wood (1994) adopted the model of Brice (1975) who developed equations describing the strain energy stored in an isotropic crystal lattice when a cation of radius r_i substitutes for the host cation of radius r_o. It was shown that partitioning of 1+, 2+ and 3+ cations between plagioclase and melt and between clinopyroxene and melt could quantitatively be described in terms of these strain energies of substitution. Beattie (1994), applying the theoretical model of Nagasawa (1966), arrived at a similar conclusion for trace element partitioning between olivine and melt. In the case of plagioclase, Blundy and Wood (1994) found that the variations of strain energy with charge bear a simple and predictable relationship to the bulk elastic properties of end-member anorthite and albite.

In order to develop a predictive model for partitioning of REE between clinopyroxene and silicate melt, we need to join a thermodynamic description of crystal and liquid properties to the strain energy model of Brice (1975) and Blundy and Wood (1994), since the latter applies only at fixed temperature, pressure and bulk

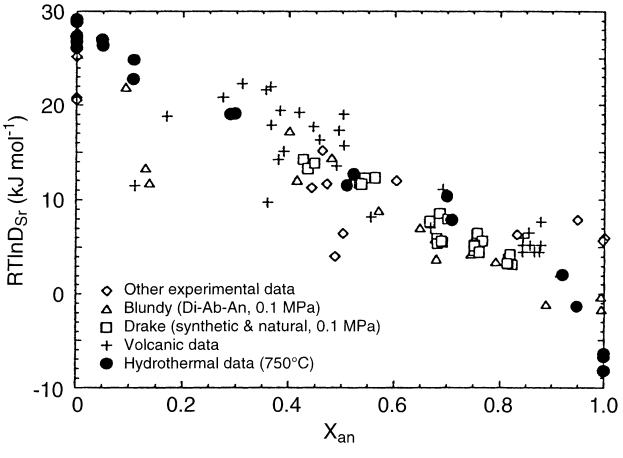

Fig. 1 Plot, taken from Blundy and Wood (1991), of $RT \ln D_{Sr}$ for plagioclase-melt partitioning as a function of mole fraction anorthite (X_{An}) in the crystal. Note that Sr is more compatible in albite ($RT \ln D_{Sr} > 0$) than in anorthite ($RT \ln D_{Sr} < 0$). Note also that the isothermal (750 °C) plagioclase-hydrothermal fluid partitioning data of Lagache and Dujon (1987) (*solid circles*) are in excellent agreement with the polythermal plagioclase-melt data. Sources of volcanic and experimental data given in Blundy and Wood (1991), except J.D. Blundy (unpublished) and Drake (1972)

(major element) composition. In order to maintain a general approach, it is necessary to consider both homovalent (e.g. Sr^{2+} for Ca^{2+}) and heterovalent (Na^{+} or REE^{3+} for Ca^{2+}) substitution. We begin with the case of homovalent substitution.

Theoretical development

Consider a hypothetical C2/c clinopyroxene $J^{2+}MgSi_2O_6$ where J^{2+} is a cation of radius r_o which fits exactly into the large M2 site without straining the structure. The partitioning of J between crystal and silicate melt should then be determined principally by the free energy of the fusion reaction:

$$\underset{\text{clinopyroxene}}{J\text{MgSi}_2\text{O}_6} = \underset{\text{melt}}{J\text{MgSi}_2\text{O}_6} \quad (1)$$

The equilibrium constant K_o is given by the simple relationships:

$$\Delta G_J^o = G^o_{J\text{MgSi}_2\text{O}_6\ \text{melt}} - G^o_{J\text{MgSi}_2\text{O}_6\text{cpx}}$$

$$K_o = \frac{a^{\text{melt}}_{J\text{MgSi}_2\text{O}_6}}{a^{\text{cpx}}_{J\text{MgSi}_2\text{O}_6}} = \exp\left(\frac{-\Delta G_J^o}{RT}\right) \quad (2)$$

where $a^{\text{cpx}}_{J\text{MgSi}_2\text{O}_6}$ and $a^{\text{melt}}_{J\text{MgSi}_2\text{O}_6}$ refer to the activity of the $J\text{MgSi}_2\text{O}_6$ component in the clinopyroxene and melt phases respectively. Given activity-composition models for melt and pyroxene, it should be possible to relate K_o to the measured Nernst partition coefficient D_o, defined as:

$$D_o = \frac{[J]_{\text{cpx}}}{[J]_{\text{melt}}} \quad (3)$$

where $[J]_{\text{cpx}}$ and $[J]_{\text{melt}}$ refer to weight fractions of J^{2+} in clinopyroxene and melt respectively.

Before attempting directly to connect D_o to K_o let us consider the effect of replacing J^{2+} in crystal and melt by very small amounts of cation I^{2+} of the same charge, but different radius r_i. Equilibrium of I^{2+} between melt and crystal can be represented in an analogous way to that outlined for $J\text{MgSi}_2\text{O}_6$ above:

$$\underset{\text{clinopyroxene}}{I\text{MgSi}_2\text{O}_6} = \underset{\text{melt}}{I\text{MgSi}_2\text{O}_6} \quad (4)$$

In this case, however, the $I\text{MgSi}_2\text{O}_6$ component is at infinite dilution in a host of essentially pure $J\text{MgSi}_2\text{O}_6$. We will assume that if I and J had exactly the same ionic radius then the standard free energy change of reactions (1) and (4) would be the same. The actual difference between the standard free energy changes is assumed to be due to the work done in straining crystal and melt by introducing a cation which is not the same size as the site. This is a reasonable assumption for closed-shell ions such as Ca^{2+}, Sr^{2+} and Mg^{2+} and it also appears to work in those cases, such as the lanthanides, where crystal field effects are small (Blundy and Wood 1994). Given this assumption the standard free energy change of reaction (4) ΔG_I^o, with I infinitely dilute in both phases, is related to that of reaction (1) by:

$$\Delta G_I^o = \Delta G_J^o + \Delta G^{\text{melt}}_{\text{strain}} - \Delta G^{\text{cpx}}_{\text{strain}} \quad (5)$$

In equation (5), $\Delta G^{\text{melt}}_{\text{strain}}$ and $\Delta G^{\text{cpx}}_{\text{strain}}$ refer to the strain energies produced by replacing one mole of J with one mole of I in an infinite volume of pure $J\text{MgSi}_2\text{O}_6$ melt and clinopyroxene respectively.

If we assume, following Blundy and Wood (1994), that the strain energy term for the melt is negligible with respect to that for the crystal, then we find the following relationship between the equilibrium constants for reactions (1), K_o, and (4), K_i:

$$K_i = \frac{a^{\text{melt}}_{I\text{MgSi}_2\text{O}_6}}{a^{\text{cpx}}_{I\text{MgSi}_2\text{O}_6}} = \exp\left(\frac{-\Delta G_J^o + \Delta G^{\text{cpx}}_{\text{strain}}}{RT}\right) = K_o \exp\left(\frac{\Delta G^{\text{cpx}}_{\text{strain}}}{RT}\right) \quad (6)$$

Equation (6) shows how the free energy relationships for trace element melting reactions should be related to those for the host cation, given our assumption that strain energy terms dominate. In order to relate the equilibrium constant K_i to partition coefficient D_i for trace element I we take the activity coefficient for $J\text{MgSi}_2\text{O}_6$ in the crystal to be a constant near 1.0 (Raoult's Law region) and assume that the activity coefficients for $I\text{MgSi}_2\text{O}_6$ and $J\text{MgSi}_2\text{O}_6$ in the melt are identical. This gives a proportionality between D_o and K_o that depends on $\gamma^{\text{melt}}_{J\text{MgSi}_2\text{O}_6}$, the activity coefficient of $J\text{MgSi}_2\text{O}_6$ in the melt, and a correction factor for mean molecular weights of melt and crystal:

$$D_o = \frac{\gamma^{\text{melt}}_{J\text{MgSi}_2\text{O}_6} \cdot \{\text{melt}\}}{K_o \cdot \{\text{crystal}\}} \quad (7)$$

where {melt} and {crystal} refer to the mean molecular weights of melt and crystalline phases respectively on a 6-oxygen basis. In a later section we introduce activity-composition models for the melt, wherein the terms $\gamma^{\text{melt}}_{I\text{MgSi}_2\text{O}_6}$ and $\gamma^{\text{melt}}_{J\text{MgSi}_2\text{O}_6}$ approach unity and can therefore be neglected (see below). Given these assumptions, the relationship between K_o and K_i (Eq. 6) can be converted into a relationship between D_o and D_i as follows:

$$D_i = D_o \exp\left(\frac{-\Delta G^{\text{cpx}}_{\text{strain}}}{RT}\right) \quad (8)$$

For a spherical site the strain-free energy term depends (Brice 1975) on the site radius r_o, the radius of the substituting ion I, r_i, and on the Young's Modulus of the site, E_S. Although the clinopyroxene M2 site is far from spherical, having 4 oxygens at 2.36 Å distance from the cation, 2 at 2.56 Å and 2 at 2.72 Å (Smyth and Bish 1988) we will follow Blundy and Wood (1994) and assume that r_o is an "equivalent" spherical radius which corresponds to that of strain-free substitution. In that case the strain energy term is given by (Brice 1975):

$$\Delta G^{\text{cpx}}_{\text{strain}} = 4\pi E_{\text{M2}} N_A \left(\frac{r_o}{2}(r_i - r_o)^2 + \frac{1}{3}(r_i - r_o)^3\right) \quad (9)$$

where N_A is Avogadro's Number and E_{M2} is the Young's Modulus of the M2 site. Combining Eqs. (8) and (9) we obtain an approximately parabolic dependence of D_i on ionic radius, with the maximum value of D corresponding to D_o, the partition coefficient for strain-free substitution in the pyroxene M2 site:

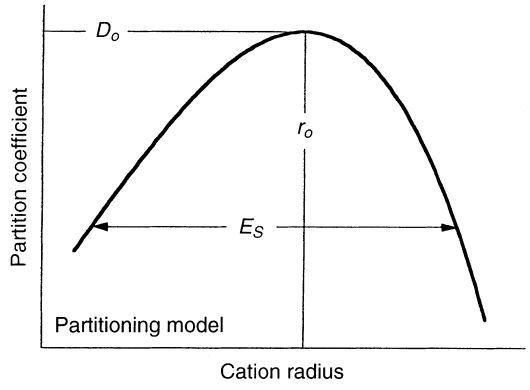

Fig. 2 A schematic showing the effects on partition coefficient of the parameters in the Brice Eq. (10). The "best-fit" ion has radius r_o and a corresponding partition coefficient D_o at the *peak* of the parabola. Partition coefficients decrease as r_i deviates in either positive or negative direction away from r_o. The derivative $\partial D/\partial r_i$ (or the "tightness" of the parabola) increases with increasing E_S, the Young's modulus of the site. D_o, and to a much lesser extent E_S, vary as a function of pressure and temperature; r_o varies primarily with crystal composition

$$D_i = D_o \exp\left(\frac{-4\pi E_{M2} N_A \left(\frac{r_o}{2}(r_i - r_o)^2 + \frac{1}{3}(r_i - r_o)^3\right)}{RT}\right) \quad (10)$$

This theoretical dependence of D_i on ionic radius, shown in Fig. 2, corresponds quite closely with observed partition coefficient values for 2+ cation substitution in both plagioclase and clinopyroxene (Blundy and Wood 1994). In each case (Figs. 3 and 4a) the peak of the curve

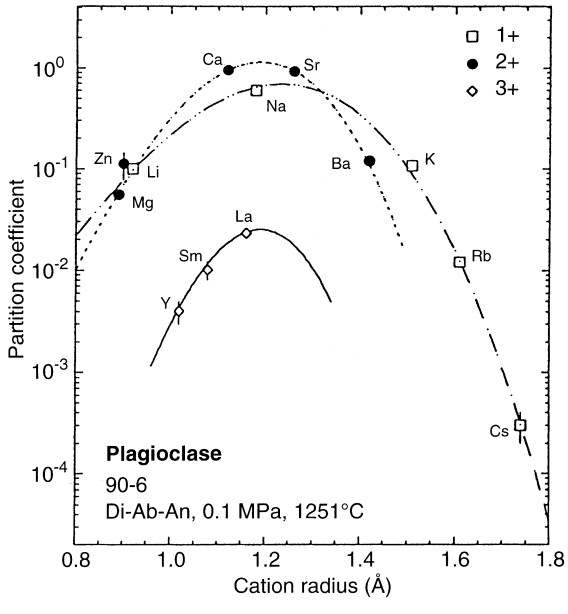

Fig. 3 Brice model fits to 1+, 2+ and 3+ cation partitioning between plagioclase (An_{89}) and silicate melt in the system diopside-albite-anorthite (Blundy and Wood 1994). Note that the best-fit curves become tighter as the charge on the cation increases from 1+ through 3+. This is due to increase in effective Young's Modulus of the site with increasing charge (see text)

is in good agreement with the site radius, and the estimated value of the Young's Modulus of the site E_S, approximates that of the bulk Ca-end-member crystal, anorthite or diopside. It is clear, therefore, that homovalent trace element substitution for Ca^{2+} in pyroxene and plagioclase follows the Brice Eq. (10) and that knowledge of the crystal-melt partitioning of, for example Ca, enables partitioning of the other 2+ ions to be predicted accurately. The height of the peak, D_o depends on K_o which means that it must depend on pressure and temperature in a predictable manner. Before addressing D_o in more detail we will consider estimation of E_S and r_o for the case of heterovalent substitution.

Determination of E and r_o

Rare earth elements in the 3+ oxidation state have similar ionic radii to Ca^{2+} and are found to substitute much more readily into Ca-rich pyroxenes than into Ca-poor pyroxenes (Jones 1995), indicating that they replace Ca^{2+} in the M2 site. Given that REE enter the M2 site, one would anticipate that their crystal-liquid partition coefficients should, like the 2+ ions, depend on the elastic properties of the crystal. For plagioclase, Blundy and Wood (1994) found that the apparent value of E_s^{2+}, derived by fitting Eq. (10) to partitioning data (Fig. 3) is twice the best-fit value of E_s^{1+} and approximately 0.6 times the value of E_s^{3+}. Furthermore, the best-fit values of E_s^{1+} and E_s^{2+} correspond closely, throughout the plagioclase series, to those of pure albite and pure anorthite respectively.

Experiments on clinopyroxene-liquid partitioning performed by Blundy and Wood (1994) and Hauri et al. (1994) show a dependence of 1+, 2+ and 3+ cation partitioning on ionic radius and charge (Fig. 4) which is similar to that observed in the plagioclase series. Some deviation from the Brice curve, also noted by Blundy and Wood (1994), can be seen in the cases of non-spherical ions such as Pb^{2+}, with its lone pair of electrons, and in transition elements such as Mn and Ni where electronic effects may be important. In general, however, closed-shell ions and lanthanides partition in accordance with the Brice model. As can be seen from Fig. 4, the D-r_i curves become tighter as cation charge increases from 1+ to 3+ demonstrating, as for plagioclase, that $E_{M2}^{1+} < E_{M2}^{2+} < E_{M2}^{3+}$. The exact relationship is more difficult to determine, however, because for $r_i \lesssim 0.95$ Å (in VIII co-ordination), cations start to enter the M1 site in clinopyroxene. This means that unequivocal M2-liquid partitioning data cannot be obtained for cations such as Li^+, Mg^{2+} and Sc^{3+} and hence that the D-r_i curves cannot be as well-constrained as for plagioclase. Some indication of the relationships between E_{M2}^{1+}, E_{M2}^{2+} and E_{M2}^{3+} may, however, be derived from observed dependencies of elastic moduli on charge in simple compounds and in cation polyhedra.

Anderson and Anderson (1970) showed that, for an ionic crystal with electrostatic attractive forces and a

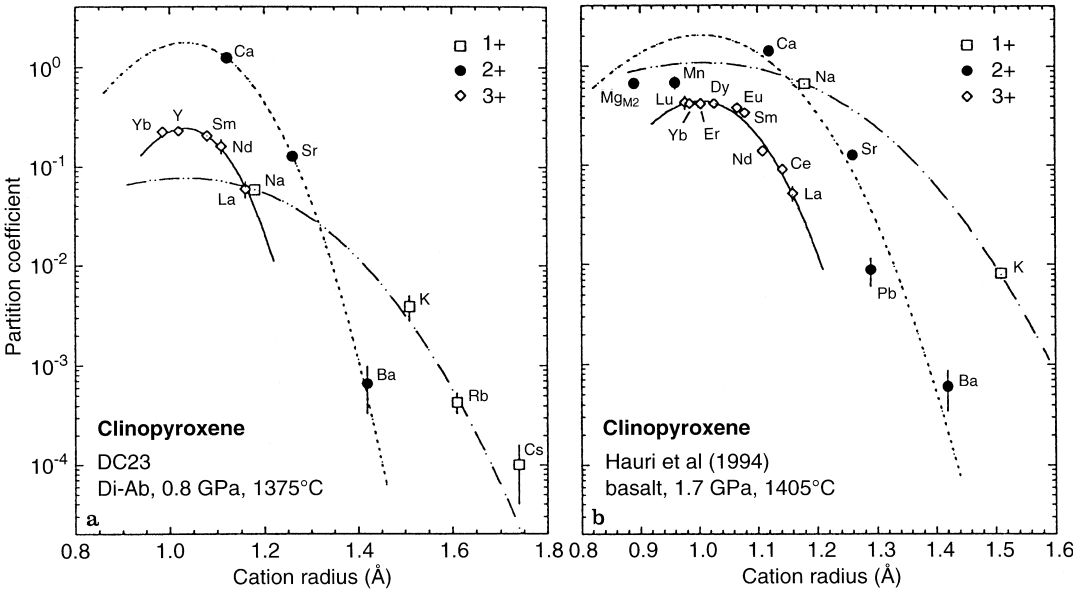

Fig. 4a,b Brice model fits to experimental data on clinopyroxene-melt partitioning: **a** clinopyroxene ($Di_{91.6}En_{7.2}Jd_{1.2}$) and silicate melt in the system diopside-albite (J.D. Blundy and J.A. Dalton, unpublished data); **b** clinopyroxene ($Mg\#_{cpx} = 0.86$) and high-alumina basaltic melt (Hauri et al. 1994). Note that the dependence of partitioning on charge is similar to that for plagioclase (Fig. 3). Deviations of Pb^{2+} and Mn^{2+} from the best-fit curves in **b** may be related to their electronic structures (see text). In **b** the Mg content of the clinopyroxene M2-site (Mg_{M2}) is calculated from the structural formula

Born power-law repulsive potential, the bulk modulus K is given by:

$$K = \frac{AZ_aZ_ce^2(n-1)}{9d_oV_o} \tag{11}$$

where V_o is the molecular volume, A is the Madelung Constant, Z_a and Z_c are the anion and cation valences respectively, e is the charge on the electron, n is the Born power-law exponent and d_o is the interatomic separation. This equation demonstrates a linear dependence of bulk modulus on cation charge for fixed structure type and molecular volume. Anderson and Anderson (1970) were able to go further and showed that a wide range of oxides with different structure types obeys the empirical relationship:

$$K = 15.7(\pm 0.5)\frac{Z_oZ_ce^2}{V_o}\ \text{GPa}$$

where Z_o is the charge on the oxygen anion. This relationship means that, in oxides, the bulk modulus is a linear function of cation charge and is inversely proportional to volume, or to the cube of the interatomic distance (in Å).

Extension of these relationships to individual cation-anion polyhedra was made by Hazen and Finger (1979) who found, for cations co-ordinated by oxygen in silicates and oxides, the following relationship (illustrated in Fig. 5):

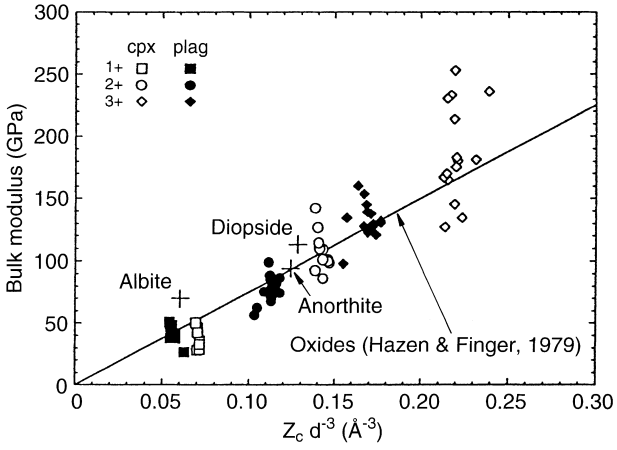

Fig. 5 Plot of bulk modulus versus cation charge (Z_c) divided by metal-oxygen distance cubed (Å^3) for cation polyhedra in oxides (Hazen and Finger 1979) and for 1+, 2+ and 3+ ions in the M2 site of clinopyroxene (this study), and the cation site in plagioclase (Blundy and Wood 1994). Note that the linear correlation derived from compressibility data by Hazen and Finger (*solid line*) holds reasonably well in our results independently estimated from the r_i-dependence of cation partition coefficient (e.g. Figs. 3 and 4). *Crosses* denote the bulk moduli of the end-member minerals albite, anorthite and diopside

$$K = 750(\pm 20)Z_cd^{-3}\ \text{GPa} \tag{12}$$

where d is the cation-anion distance, equivalent to r_o plus the radius of the oxygen anion, $r_{O^{2-}}$ (= 1.38 Å; Shannon 1976), and Z_c is the cation charge. The bulk modulus K is therefore observed to be a linear function of cation charge in oxides and in oxygen polyhedra of the kind we are concerned with in clinopyroxene. To extend the observed correlation to Young's modulus, E, we need to consider the identity relating E and K:

$$E = \frac{3K}{1-2\sigma}$$

where σ is Poisson's ratio. Most minerals approximate Poisson solids and in this case, when $\sigma \approx 0.25$ we obtain:

$$E \approx 1.5\ K \tag{13}$$

Therefore the value of E_S in Eq. (10) should, like bulk modulus, be an approximately linear function of cation charge. This is exactly what we observed previously (Blundy and Wood 1994) for plagioclases, where 1+, 2+ and 3+ values of the Young's Modulus of the large cation site were found to be 67, 128.5 and 190 GPa respectively for anorthite and 52, 104 and 198 GPa for albite. When converted to site bulk modulus using Eq. (13) we find, as shown in Fig. 5, that the elastic properties of the large cation site in plagioclase calculated from trace element partitioning are in very good agreement with the empirical relationship derived by Hazen and Finger (1979) from observed compressibilities of oxide polyhedra in minerals. Furthermore, the values obtained from trace element partitioning are, for 1+ and 2+ ions, in excellent agreement with the bulk properties of albite and anorthite respectively, suggesting that the bulk elastic properties are controlled, in this case, by the large cation site.

Turning to Ca-pyroxene, we find that the room temperature bulk modulus of pure diopside, 113 GPa (Sumino and Anderson 1984), when scaled to the size and charge of the M2 site, is also in good agreement with the Hazen and Finger relationship (Fig. 5). This suggests that one may be able to use Eq. (12) to estimate the effective values of E^{3+}_{M2} for the pyroxene M2 site. However, instead of forcing a value of E^{3+}_{M2} on the pyroxene REE partitioning data we first attempted to estimate E^{3+}_{M2} and r_o directly in cases where there were sufficient data. That is, we took experiments where four or more REE partition coefficients were simultaneously measured (Grutzeck et al. 1974; McKay et al. 1986; Hart and Dunn 1993; Hauri et al. 1994; and J.D. Blundy, 6 unpublished points) and fitted Eq. (10) to each experiment in turn using a general non-linear fitting routine (Press et al. 1986, p. 526). The results of Hart and Dunn (1993) cover the entire range of REE radii and show that r_o has a peak at about the radius of Ho, 1.015Å, with an estimated value of E^{3+}_{M2} of 280($\pm$50) GPa corresponding to a K^{3+}_{M2} value of about 187 GPa. The data of Hauri et al. (1994) (Fig. 4) show similar trends, with a plateau in D for REE with ionic radii between 0.977 and 1.027Å and K values of 145–215 GPa. In all, 16 sets of data were treated in this way and the results for E^{3+}_{M2}, converted into K^{3+}_{M2}, are plotted on Fig. 5. In Fig. 5, fitted values of r_o were converted to d, by adding 1.38Å for the radius of the oxygen anion. As can be seen, the results are scattered, but the average, about 180 GPa, lies quite close to the line of Hazen and Finger (1979). The reason for the scatter is that fit-values of E^{3+}_{M2} and r_o are highly correlated, so that, in those cases where r_o is not very well constrained by the data, small errors in D value propagate into large, correlated errors in r_o and E^{3+}_{M2}.

Because of the scatter in E^{3+}_{M2} values we made no attempt to fit the site modulus to an equation in temperature, pressure or pyroxene composition. Instead, noting that E^{3+}_{M2} is close to what would be predicted from Eqs. (12) and (13) we constrained it to have a value corresponding to K^{3+}_{M2} of 180 GPa under P-T conditions close to the average used in the experiments i.e. at about 1.5 GPa and 1650 K. Under these conditions the difference in the bulk-crystal Young's Modulus of diopside and enstatite is only 12% relative (Anderson 1989, p. 105). We therefore assumed that E^{3+}_{M2} is independent of composition. We assumed further, from Eq. (13), that the temperature and pressure derivatives of E^{3+}_{M2} would bear a simple relationship to the temperature and pressure derivatives of the elastic properties of diopside. This follows from Eq. (12) and the observed relationship between the bulk modulus of diopside and the bulk modulus of the M2 site:

$$E^{3+}_{M2} = 1.5E^{2+}_{M2} \approx 1.5E_{\mathrm{Diop}}$$

Then, assuming that this relationship holds over all of pressure-temperature space, we obtain:

$$\left(\frac{\partial E^{3+}_{M2}}{\partial T}\right)_P = 1.5\left(\frac{\partial E_{\mathrm{Diop}}}{\partial T}\right)_P$$

and

$$\left(\frac{\partial E^{3+}_{M2}}{\partial P}\right)_T = 1.5\left(\frac{\partial E_{\mathrm{Diop}}}{\partial P}\right)_T$$

Using the temperature and pressure derivatives of the bulk and shear moduli of diopside tabulated by Anderson (1989) and constraining the average E^{3+}_{M2} for experimental P-T conditions as above, we arrived at the following equation for 3+ cation substitution into the clinopyroxene M2 site:

$$E^{3+}_{M2} = 318.6 + 6.9P - 0.036T\ \mathrm{GPa} \tag{14}$$

where P is in GPa and T in Kelvin.

Given this expression for E^{3+}_{M2} we then used the non-linear fitting program to derive values of r_o from a total of 82 experiments in which 3 or more pyroxene-liquid REE partition coefficients were measured and in which the compositions of crystal and liquid phases were well constrained. These comprised 11 of the experiments discussed above, 25 experiments of Hack et al. (1994), 37 experiments described by Gallahan and Nielsen (1992) and a further 9 unpublished points of Blundy, which are described briefly in Blundy and Wood (1994). Adopted radii values for individual REE were those of Shannon (1976) for 3+ ions in VIII co-ordination. Resulting values of r_o range from 0.979 to 1.055 Å. A similar range in optimum M2 site radius was obtained by Liu et al. (1992) who ascribed the variations to the effect of pressure. However, as noted by Liu et al., pressure is strongly correlated with crystal composition in clinopyroxene, particularly with Na and Al content. We performed stepwise linear regression of the derived values of r_o against all major compositional parameters, pressure and temperature. The result is that the only important parameters are the Al content of the M1 site, and the Ca content of the M2 site. All other parameters,

including pressure, have $F < 0.6$ and cannot be considered significant. We find that the following equation fits the 82 points with a standard deviation of 0.009 Å (i.e. less than the difference in ionic radius between adjacent REE):

$$r_o = 0.974 + 0.067X_{Ca}^{M2} - 0.051X_{Al}^{M1}\text{Å} \quad (15)$$

The derived dependence of r_o on X_{Al}^{M1} (-0.051Å) is consistent with crystal-chemical data on the change in M2 site radius on going from $CaMgSi_2O_6$ to $CaAl_2SiO_6$ (Smyth and Bish 1988) and with REE partitioning data in the system CaO-MgO-Al_2O_3-SiO_2 (Blundy et al. 1996) which give -0.04Å per Al atom in M1. For those experiments where there were 3 or more data points on 2+ ions (11 experiments) or on 1+ ions (9 experiments), we then used the r_o values obtained from the REE partition coefficients to derive E_{M2}^{2+} and E_{M2}^{1+} values using the fitting program. These were converted to K values using Eq. (13) and are also shown in Fig. 5. Figure 5 demonstrates that the 1+, 2+ and 3+ ions obey the Hazen and Finger (1979) relationship approximately, but that the slope of the curve is slightly higher for pyroxene. Nevertheless, the general trend of the data is in accord with the suggestion that the effective E value for the clinopyroxene M2 site is a linear function of the charge on the substituting cation.

A test of the applicability of Eqs. (14) and (15) to REE substitution in clinopyroxene is provided by their ability to predict the partition coefficient of element G, D_g, from the value for element I, D_i. Most of the studies in the literature involved measurement of one of the middle REE such as Sm and Gd. We used Eqs. (14), (15) and (10) to predict r_o, E_{M2}^{3+} and D_o^{3+} for each of these experimental data then used the measured D_{Sm} or D_{Gd} to predict the partition coefficients for the other REE and Y. These were compared with the measured values (251 total points) and are represented in Fig. 6 as:

$$\text{Error } (J) = RT \ln\left(\frac{D_g^{calc}}{D_g^{obs}}\right)$$

The standard deviation of 2762 J corresponds to an error in D_j^{calc} of about 24%. Less than 45% of the experimental data were used to fit Eq. (15) for r_o, so this is a true test of predictive capability. Several observations should be made. Firstly, that the experimental data are overwhelmingly of electron-microprobe (EMP) origin and that the 1σ uncertainty in D_j from EMP analysis is typically 20–50%. Therefore our equations predict the data to within experimental uncertainty. Secondly, the 1σ error in La is typically of the order of 50% (Gallahan and Nielsen 1992) and of our 251 points, 72 are predictions for La which has increased the scatter in the results. (Note that for 47 of these from Gallahan and Nielsen (1992) Y was used as the predictor because Sm and Gd data were not available). Finally, 92% of the data lie between ± 4000 J in error corresponding to a predicted partition coefficient of between 0.73 and 1.36 times the measured value. Since this is within the uncertainty in EMP determinations of D, we consider that the effects of crystal composition and ionic radius on D_{REE} for clinopyroxene are now fully constrained. In any experiment all that is now required is accurate measurement of one middle REE partition coefficient and crystal bulk composition. Equations (10), (14) and (15) can then be used to calculate r_o, E_{M2}^{3+} and D_o^{3+} and to predict the partition coefficients for the other REE or for any other 3+ ion which enters the M2 site (e.g. Cm^{3+}, Am^{3+}).

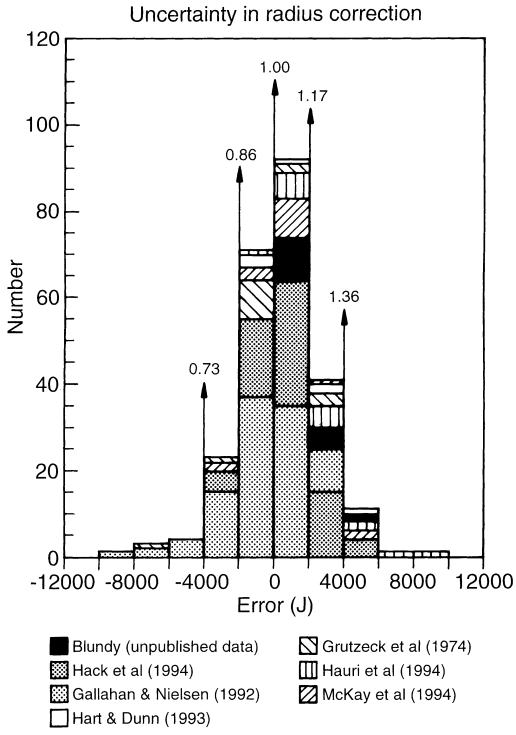

Fig. 6 Histogram of 251 points showing the error in $RT \ln D_{REE}$ which arises when the measured D for one middle REE is used, through Eqs. (10), (14) and (15), to calculate the other D_{REE} values under the same conditions. Values on *arrows* denote equivalent fractional deviation from the true value at 1523 K. More than 92% of calculated D_{REE} values are within the uncertainties in experimental measurement (see text)

Having established the validity of Eqs. (10), (14) and (15) we can now calculate r_o, E_{M2}^{3+} and D_o^{3+} for all available REE partition coefficient data. We performed this for 481 data points in the literature for which the partition coefficients were measured using a microbeam technique, either EMP or ion microprobe. The data now form a matrix of points in pressure-temperature-composition space in which the effects of ionic radius and crystal composition have been removed. This means that, if one could correct for activity-composition relations of the melt phase, then, at fixed pressure and temperature, all experiments, regardless of bulk composition and REE studied, should give the same value of D_o. The next step is to attempt to correct for compositional effects in the melt phase.

A melt model

Structurally, aluminosilicate melts are known to be complex, containing a variety of anionic species having only a resemblance to, rather than an equality with, the structures of the liquidus solid phases (e.g. Mysen 1990). Despite this complexity it appears that, over certain compositional ranges, silicate melts may behave thermodynamically as if they contained simple ordered structural units (Burnham 1981; Blundy et al. 1995). In the absence of complete speciation data, we attempted to take advantage of these latter observations as a means of systematising the dependence of partition coefficients on silicate melt composition. Before considering REE, we use the same approach to investigate thermodynamically better constrained equilibria.

Blundy et al. (1995) investigated the partitioning behaviour of sodium between clinopyroxene and silicate melts over a wide range of pressure and temperature. They showed that the crystal-liquid partition coefficient D_{Na} bears a very simple relationship to the equilibrium constant K_{Na} for the melting reaction:

$$\underset{\text{crystal}}{NaAlSi_2O_6} = \underset{\text{melt}}{NaAlSi_2O_6} \tag{16}$$

Taking standard states of crystal and melt phase to be pure $NaAlSi_2O_6$ crystal and liquid respectively at the P, T of interest then K_{Na} is related to the standard state free energy change of the melting reaction, ΔG^o_{fusion}:

$$\Delta G^o = -RT \ln K_{Na} = -RT \ln \left(\frac{a^{melt}_{NaAlSi_2O_6}}{a^{cpx}_{NaAlSi_2O_6}} \right) \tag{17}$$

Blundy et al. then converted activities to composition using the observation of Holland (1990) that $a^{cpx}_{NaAlSi_2O_6}$ at low $X^{cpx}_{NaAlSi_2O_6}$ is approximately equal to X^{M2}_{Na}, the mole fraction of sodium on the M2 site in clinopyroxene, i.e.

$$a^{cpx}_{NaAlSi_2O_6} = \text{number of Na atoms per 6 oxygens} \tag{18}$$

For the melt Blundy et al. (1995) used exactly the same assumption:

$$a^{melt}_{NaAlSi_2O_6} = \text{number of Na atoms per 6 oxygens} \tag{19}$$

This is equivalent to a quasicrystalline melt model (Burnham 1981) in which the melt is assumed to consist of pyroxene-like units. If this simplification is a reasonable assumption, then ΔG^o can be related to D_{Na}, the crystal/liquid partition coefficient, through Eq. (7). Given that the difference in mean molecular weight between crystal and liquid (generally less than 3%) can be ignored, we obtain:

$$\Delta G^o = RT \ln(D_{Na}) \tag{20}$$

Although the melt model is a gross simplification, Blundy et. al (1995) found that the standard state free energy change of the melting reaction derived from calorimetric and phase equilibrium data on pure $NaAlSi_2O_6$ is in excellent agreement with the sodium partitioning data for a wide range of synthetic and natural compositions (Fig. 7). The data shown in this figure span a wide composition range from the diopside-albite join to natural tholeiite and picrite, over a pressure and temperature range of 0.1 MPa to 6 GPa and 1097–1800 °C respectively. This means that the simple activity-composition relationship for $NaAlSi_2O_6$ in melt (19) gives a reasonable representation of the partial molar free energy of the $NaAlSi_2O_6$ component over most of the pressure, temperature and compositional ranges of importance in petrology. The only compositions which deviate from the simple activity-composition relationships are those containing substantial $NaFe^{3+}Si_2O_6$ component, and those on the diopside-albite join where the SiO_2 content is high enough for non-ideal $CaMgSi_2O_6$-SiO_2 interactions to interfere (Blundy et al. 1995). In basaltic and picritic compositions, however, the simple melt and crystal models enable thermodynamic data on pure $NaAlSi_2O_6$ to be used to calculate D_{Na} within 17% for pressures of 1 GPa and above. This means that one point on the D-r_i curve for 1+ cations can be determined accurately at any pressure and temperature. Then, from Eqs. (10), (14), (15) the remainder of the curve may be calculated for larger univalent ions such as K^+, Rb^+ and Cs^+, given a suitable value for E^{1+}_{M2}, e.g. $0.5\,E^{2+}_{M2}$.

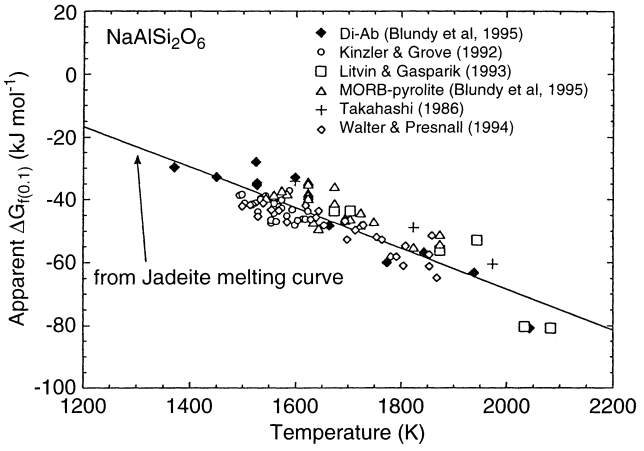

Fig. 7 The apparent 0.1 MPa free energy of fusion of jadeite, $NaAlSi_2O_6$, as a function of temperature. *Solid line* was obtained from the melting curve of pure jadeite (Blundy et al. 1995). *Points* were obtained from measured partitioning of $NaAlSi_2O_6$ component between clinopyroxene and liquid in simple and complex systems and assuming ideal solution in both phases (see text). Agreement between data for pure jadeite and those for dilute $NaAlSi_2O_6$ component assuming ideal solution confirms that ideal behaviour (i.e. $\gamma^{melt}_{NaAlSi_2O_6} = \gamma^{cpx}_{NaAlSi_2O_6} \approx 1.0$) is a reasonable assumption

Given the success of this model for Na pyroxenes, we assessed whether the same approach can be applied to the major Ca-components of igneous clinopyroxenes and, in turn to trace components containing REE and similar 3+ ions. Consider, therefore, the melting of diopside $CaMgSi_2O_6$:

$$\underset{\text{Diopside}}{CaMgSi_2O_6} = \underset{\text{Melt}}{CaMgSi_2O_6}$$

At the P, T of interest ΔG^o for this reaction is related to the ratio of activities in melt and crystalline phases through an analogous equation to (17). Along the melting curve for pure diopside the equilibrium constant is 1.0 (both phases pure), hence:

$$\Delta G^o_{PT} = \Delta H^o_{T_f} + \int_{T_f}^{T} \Delta C_p \mathrm{d}T - T\left(\Delta S^o_{T_f} + \int_{T_f}^{T} \frac{\Delta C_p}{T}\mathrm{d}T\right) + \int_{0.1}^{P} \Delta V^o \mathrm{d}P = 0$$

Or, rearranging:

$$\Delta H^o_{T_f} - T\Delta S^o_{T_f} = -\int_{T_f}^{T} \Delta C_p \mathrm{d}T + T\int_{T_f}^{T} \frac{\Delta C_p}{T}\mathrm{d}T - \int_{0.1}^{P} \Delta V^o \mathrm{d}P \qquad (21)$$

where ΔC_P, ΔS^o and so on refer to the differences in thermodynamic properties between pure melt and pure crystal, P and T refer to the pressure and temperature of interest and T_f to the fusion temperature at 0.1 MPa (1665 K). The left hand side of Eq. (21) is the free energy of fusion at 0.1 MPa with the heat capacity terms removed in order to linearise it with respect to temperature. Henceforth the term $\Delta H^o_{T_f} - T\Delta S^o_{T_f}$ will be referred to as the "apparent 0.1 MPa free energy of fusion". The integrals on the right hand side of Eq. (21) were evaluated along the diopside fusion curve of Williams and Kennedy (1969) to 5 GPa. Data for heat capacity for diopside crystals were taken from Robie et al. (1979) and for diopside melt from Lange and Carmichael (1990). Liquid volume data were obtained from Lange and Carmichael (1990) and crystal volume data as a function of temperature from Finger and Ohashi (1976). Bulk modulus data for diopside were taken from the summary of Anderson (1989) while liquid compressibilities came from Lange and Carmichael (1990). The pressure integral was evaluated from the Birch-Murnaghan equation using integration by parts (see Blundy et al. 1995).

The terms on the right hand side of Eq. (21), calculated from the diopside fusion curve, are shown as a function of temperature (crosses) in Fig. 8. The slope of the curve should yield the ΔS^o of fusion at T_f. The calorimetric value of $\Delta S^o_{T_f}$, $82.5 \pm 1.2\,\mathrm{J\,mol^{-1}\,K^{-1}}$ (Richet and Bottinga 1986), is in excellent agreement with value obtained by regression, $83.4\,\mathrm{J\,K^{-1}}$ at 1665 K, indicating that derived values of enthalpy, entropy and heat capacity changes of the fusion reaction to 5 GPa are all internally consistent. If good models of activity-composition relations for solid and liquid phases can be obtained, then, as previously shown for jadeite, calculated equilibrium constants for coexisting clinopyroxene and liquid in complex systems should be consistent with the results extracted from the diopside fusion curve.

We took experimental data on basaltic and haplobasaltic liquids at high pressure and temperature from Walter and Presnall (1994), Kinzler and Grove (1992), and Blundy et al. (1995, appendix). These data apply to approximately basaltic liquids and span a wide P-T range (0.7–3.5 GPa, 1493–1873 K). For each experimental point we calculated the activity of $CaMgSi_2O_6$ component in the crystal using the 2-site ideal model (Wood and Banno 1973):

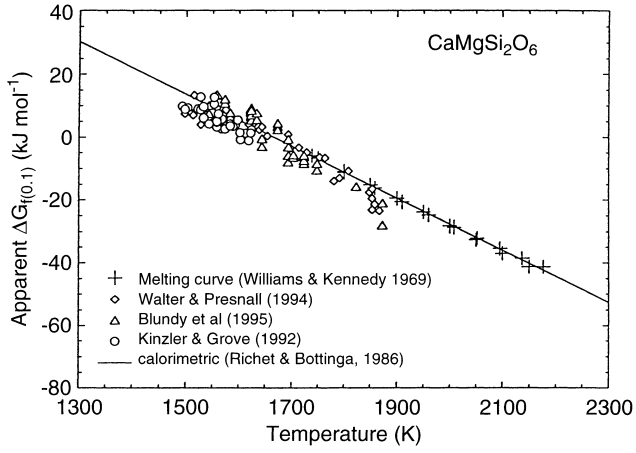

Fig. 8 The apparent 0.1 MPa free energy of fusion of diopside, $CaMgSi_2O_6$, as a function of temperature. *Solid line* is the calorimetric measurements of Richet and Bottinga (1986), while *crosses* are values extracted from the melting curve of pure diopside measured by Williams and Kennedy (1969). All other *points* are from high pressure experiments on basaltic and related systems and were calculated by assuming ideal mixing of $CaMgSi_2O_6$ component in liquid and solid phases. Ideal mixing (i.e. $\gamma^{\mathrm{melt}}_{CaMgSi_2O_6} = \gamma^{\mathrm{cpx}}_{CaMgSi_2O_6} \approx 1.0$) appears, over this composition range, to be a reasonable assumption

$$a^{\mathrm{cpx}}_{CaMgSi_2O_6} = X^{\mathrm{M2}}_{\mathrm{Ca}} \cdot X^{\mathrm{M1}}_{\mathrm{Mg}} \qquad (22)$$

where $X^{\mathrm{M2}}_{\mathrm{Ca}}$ and $X^{\mathrm{M1}}_{\mathrm{Mg}}$ refer to atomic fractions of Ca and Mg on the clinopyroxene M2 and M1 sites, respectively, calculated using the method of Wood and Banno (1973). For the melt we used a quasicrystalline model in which the melt analysis is recast as the 6-oxygen components: $NaAlSi_2O_6$, $KAlSi_2O_6$, $CaTiAl_2O_6$, $CaAl_2SiO_6$, $(Mg,Fe)_3Si_{1.5}O_6$, Si_3O_6 and $Ca(Mg,Fe)Si_2O_6$. Calculation of the components is straightforward (see Appendix) and provides the potential for CIPW-normative olivine, quartz and nepheline as well as hypersthene. We then obtained an estimate of $CaMgSi_2O_6$ activity from the mole fraction of $Ca(Mg,Fe)Si_2O_6$ component and the molar ratio of Mg to Mg + Fe ($Mg\#_{\mathrm{melt}}$):

$$a^{\mathrm{cpx}}_{CaMgSi_2O_6} = X^{\mathrm{melt}}_{Ca(Mg,Fe)Si_2O_6} \cdot Mg\#_{\mathrm{melt}} \qquad (23)$$

This activity model is equivalent to that employed by Blundy et al. (1995) for $NaAlSi_2O_6$ component in silicate melt. For each experimental point we calculated an apparent 0.1 MPa free energy of fusion from Eq. (21) with the activity terms on the right hand side to take account of mixing:

$$\Delta H^o_{T_f} - T\Delta S^o_{T_f} = -\int_{T_f}^{T} \Delta C_p \mathrm{d}T + T\int_{T_f}^{T} \frac{\Delta C_p}{T}\mathrm{d}T - \int_{0.1}^{P} \Delta V^o \mathrm{d}P - RT\ln\left(\frac{a^{\mathrm{melt}}_{CaMgSi_2O_6}}{a^{\mathrm{cpx}}_{CaMgSi_2O_6}}\right) \qquad (24)$$

Results, shown in Fig. 8, demonstrate that, as with $NaAlSi_2O_6$, the simple activity-composition relations produce good agreement between the fusion curve of pure diopside and the partitioning of $CaMgSi_2O_6$ component between clinopyroxene and silicate melt for a wide range of bulk compositions. Calculated values only begin to deviate from the predicted curve under high P-T conditions (> 1800 K and > 3 GPa) where the normative olivine contents of the liquids are greater than 40%.

Although the good agreement between predicted and observed partitioning implies that basaltic liquids saturated in clinopyroxene are structurally similar to diopside liquid, we emphasise that this is certainly not required by our observations. All we have shown is that, assuming basaltic liquids have pyroxene-like stoichiometry, then the activities of $NaAlSi_2O_6$ and $CaMgSi_2O_6$ components are roughly equal to their mole fractions. Importantly this provides a means of estimating D_{Ca} and D_{Na} with good accuracy and hence fixing one point on each of the 1+ and 2+ partition coefficient curves (Fig. 2). With the r_o Eq. (15) and the bulk modulus-molecular volume relationships of Fig. 5, they provide means of calculating the full D-r_i curves for both 1+ and 2+ ions substituting on the M2 site.

Heterovalent substitution and D_o for REE

Having demonstrated that D_{Na} and D_{Ca} may, with simple activity-composition relations, be related to the free energies of fusion of pure $NaAlSi_2O_6$ and $CaMgSi_2O_6$ pyroxenes, we now consider whether or not a similar approach can work for the REE. In this case the value of D_o^{3+} for a strain-free substituent, may be obtained from Eqs. (10), (14), and (15). The main difficulty arises from the fact that no thermodynamic or melting data exist for end-member REE pyroxenes. In place of such data we need, as a minimum, a good understanding of the mechanism by which REE^{3+} substitute for Ca^{2+} on M2. There are several possibilities. The Ca substitution may be coupled to the replacement of a tetrahedral Si atom by Al, leading to a hypothetical REE pyroxene end-member $REEMgAlSiO_6$. Additional possibilities are replacement of 2Ca on M2 by Na + REE, or of 3 Ca by 2REE plus a vacancy, leading to the hypothetical end-members $Na_{0.5}REE_{0.5}MgSi_2O_6$ and $REE_{0.667}MgSi_2O_6$ respectively. In practice, all three substitutions can rigorously be described thermodynamically and are hence equally valid. Practically speaking, however, the experimental difficulties involved in obtaining the vacancy concentration on M2 make the activity of the $REE_{0.667}MgSi_2O_6$ component almost impossible to define. We will therefore confine ourselves to the components $Na_{0.5}REE_{0.5}MgSi_2O_6$ and $REEMgAlSiO_6$.

Consider a melting reaction analogous to reaction (4), but involving the component $Na_{0.5}REE_{0.5}MgSi_2O_6$:

$$\underset{\text{clinopyroxene}}{Na_{0.5}REE_{.5}MgSi_2O_6} = \underset{\text{melt}}{Na_{0.5}REE_{0.5}MgSi_2O_6} \qquad (25)$$

The enthalpy and entropy changes of this reaction at 0.1 MPa are related to the equilibrium constant (Eq. 24) as follows:

$$\Delta H^o_{T_f} - T\Delta S^o_{T_f} = -\int_{T_f}^{T} \Delta C_p \mathrm{d}T + T\int_{T_f}^{T} \frac{\Delta C_p}{T}\mathrm{d}T - \int_{0.1}^{P} \Delta V^o \mathrm{d}P - RT\ln\left(\frac{a^{\text{melt}}_{Na_{0.5}REE_{0.5}MgSi_2O_6}}{a^{\text{cpx}}_{Na_{0.5}REE_{0.5}MgSi_2O_6}}\right) \qquad (26)$$

Let us assume that liquid and solid phases obey simple activity-composition relations similar to those exhibited by $NaAlSi_2O_6$ and $CaMgSi_2O_6$ components in liquid and crystalline phases. For crystalline pyroxene in the absence of short-range order on the M-sites we would anticipate activity-composition relations of the form:

$$a^{\text{cpx}}_{Na_{0.5}REE_{0.5}MgSi_2O_6} = \left(X^{M2}_{Na}\right)^{0.5}\cdot\left(X^{M2}_{REE}\right)^{0.5}\cdot X^{M1}_{Mg}$$

while for the liquid, continuing the analogy with $NaAlSi_2O_6$ and $CaMgSi_2O_6$, we might expect:

$$a^{\text{melt}}_{Na_{0.5}REE_{0.5}MgSi_2O_6} = [\mathrm{Na}]^{0.5}\cdot[\mathrm{REE}]^{0.5}\cdot Mg\#_{\text{melt}}$$

where [Na] refers to the number of Na atoms and [REE] to the number of REE atoms per 6 oxygens.

Applying Eq. (7) and assuming that liquid and solid activity coefficients cancel we obtain:

$$\Delta H^o_{T_f} - T\Delta S^o_{T_f} = -\int_{T_f}^{T} \Delta C_p \mathrm{d}T + T\int_{T_f}^{T} \frac{\Delta C_p}{T}\mathrm{d}T - \int_{0.1}^{P} \Delta V^o \mathrm{d}P + RT\ln\left(\frac{D^{0.5}_{Na}\cdot\left(D^{3+}_o\right)^{0.5}\cdot X^{M1}_{Mg}\cdot\{\text{crystal}\}}{Mg\#_{\text{melt}}\cdot\{\text{melt}\}}\right) \qquad (27)$$

where D_o^{3+} refers to the "strain-free" partition coefficient for a rare earth element with radius r_o at the conditions of interest. Although the heat capacity differences between products and reactants are unknown, they can generally be assumed equal to zero over quite wide temperature ranges (e.g. Wood and Fraser 1976, p. 42). Once again the difference in mean atomic weight between coexisting natural liquid and clinopyroxene (0–3%) is negligible with respect to uncertainties in experimental values of D_{REE}. Therefore (27) may be simplified to:

$$\Delta H^o_{T_f} - T\Delta S^o_{T_f} = -\int_{0.1}^{P} \Delta V^o \mathrm{d}P - RT\ln\left(\frac{D^{0.5}_{Na}\cdot\left(D^{3+}_o\right)^{0.5}\cdot X^{M1}_{Mg}}{Mg\#_{\text{melt}}}\right) \qquad (28)$$

The volume change of the reaction is also unknown, and certainly cannot, because of the large volume of fusion of jadeite, 22 $cm^3\ mol^{-1}$ at atmospheric pressure (Blundy et al. 1995), be assumed equal to zero. The volume of fusion of jadeite is, however an approximately linear function of pressure to 6 GPa, which means that the integral may be simplified as follows:

$$\Delta H^o_{T_f} - T\Delta S^o_{T_f} + P\Delta V - \frac{1}{2}\left(\frac{\partial\Delta V}{\partial P}\right)P^2 = RT\ln\left(\frac{D^{0.5}_{Na}\cdot\left(D^{3+}_o\right)^{0.5}\cdot X^{M1}_{Mg}}{Mg\#_{\text{melt}}}\right) \qquad (29)$$

We calculated D_{Na} and D_o^{3+} for all data in the literature (427 points) for which sodium and REE partition coefficients had been measured using a microbeam technique. Only data for which the melt was an *anhydrous* silicate were included. We then regressed the right hand side of Eq. (29) against T, P and P^2 to estimate the entropy, enthalpy and volume of fusion of the hypothetical $Na_{0.5}REE_{0.5}MgSi_2O_6$ pyroxene. The data fit Eq. (29) with a standard deviation of 2820 J and yield a value of ΔS_T^o of $80.16\,J\,mol^{-1}\,K^{-1}$ and ΔV of fusion of $12\,cm^3\,mol^{-1}$ at 0.1 MPa. The results make thermodynamic sense in that the extrapolated volume of fusion of $Na_{0.5}REE_{0.5}MgSi_2O_6$ pyroxene at 0.1 MPa ($12\,cm^3\,mol^{-1}$) is more than half the value for jadeite. The estimated entropy of fusion is also in good agreement with values for other pyroxenes: Richet and Bottinga (1986) give $82.5\,J\,mol^{-1}\,K^{-1}$ for diopside while Blundy et al. (1995) estimate $64.8\,J\,mol^{-1}\,K^{-1}$ for jadeite.

Values of the right hand side of Eq. (29), corrected for pressure using the volume terms, were obtained for all the 427 available points of D_{REE} measured by a microbeam technique. All points, for all REE, are plotted on the same diagram as a function of temperature in Fig. 9. The validity of our radius correction is clear, as is the temperature dependence and the simple activity-composition relations we have used. The points shown in Fig. 9 have a standard deviation (2820 J) which is essentially the same as that (2840 J) obtained by Blundy et al. (1995) for partitioning of Na between pyroxene and liquid. This means that our model fits the REE data as well as the Blundy et al. (1995) model fits the Na partitioning data. It should therefore be possible to use our fit parameters, in conjunction with the Na partitioning equation of Blundy et al. (1995) to calculate

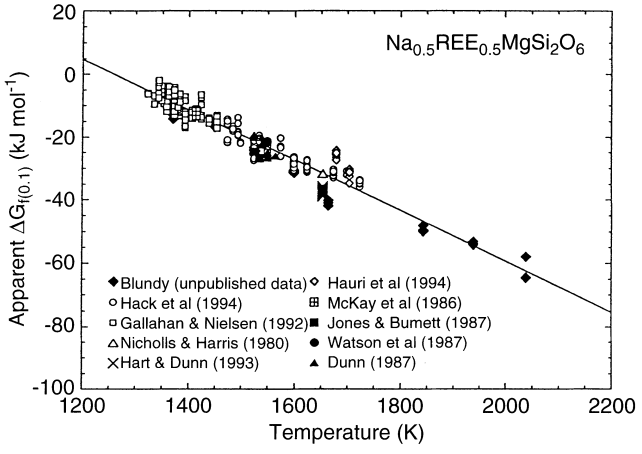

Fig. 9 The apparent 0.1 MPa free energy of fusion of hypothetical $Na_{0.5}REE_{0.5}MgSi_2O_6$ pyroxene plotted as a function of temperature. The *points* are 427 simultaneously-measured Na and REE (or Y) partition coefficients from the literature with the strain energy of REE substitution removed using Eq. (10). All REE elements are plotted on the same figure which demonstrates the validity of our radius correction and of simple ideal activity-composition relations for solid and melt phases

D_o^{3+}, and hence D_{REE} for any rare earth element, from the crystal composition. In practice, however, we find that, because of errors in measured Na contents of glass and pyroxene, a second equilibrium, that involving the $REEMgAlSiO_6$ component, produces less scatter in calculated D_{REE}.

Consider the melting reaction:

$$\underset{\text{clinopyroxene}}{REEMgAlSiO_6} = \underset{\text{melt}}{REEMgAlSiO_6} \tag{30}$$

The equilibrium constant K_o is given by the activity ratio which must be related to measured concentrations in the two phases. For the clinopyroxene we follow Blundy et al. (1996) and the experimentally determined activity-composition relations in aluminous clinopyroxenes (Wood 1987), with ideal solution on each individual sublattice, giving:

$$a^{cpx}_{REEMgAlSiO_6} = X^{M2}_{REE} \cdot X^{M1}_{Mg} \tag{31}$$

Blundy et al. (1996) considered the effect of liquid bulk composition on measured REE partition coefficients in the system CaO-MgO-Al_2O_3-SiO_2 (CMAS) at 0.1 MPa. They showed that, after correcting for crystal composition, a 2-lattice model for the liquid, one lattice containing cations such as REE^{3+} and Ca^{2+} and the other anions such as $Si_3O_6^0$, $AlSiO_6^{5-}$ and $Si_2O_6^{4-}$, could explain much of the dependence of partition coefficient on liquid composition. We attempted to extend this model to the wide range of liquid compositions used in the experiments shown in Fig. 9, but obtained very scattered results. We therefore conclude that their model is not, at this stage, generalisable outside CMAS. We therefore returned to the simple model used for $NaAlSi_2O_6$, $CaMgSi_2O_6$ and $Na_{0.5}REE_{0.5}MgSi_2O_6$ melts:

$$a^{melt}_{REEMgAlSiO_6} = [REE] \cdot Mg\#_{melt} \tag{32}$$

where [REE] refers to the atomic concentration of the REE in the melt on a 6-oxygen basis. These assumptions, again taking the ratio of mean atomic weights to be 1.0, lead to the following expression for equilibrium constant:

$$\Delta H_T^o - T\Delta S_T^o + P\Delta V - \frac{1}{2}\left(\frac{\partial \Delta V}{\partial P}\right)P^2 = RT\ln\left(\frac{D_o^{3+} \cdot X^{M1}_{Mg}}{Mg\#_{melt}}\right) \tag{33}$$

where D_o^{3+} refers, as before, to the partition coefficient of the "strain-free" REE substituent. We used 481 data points on all analysed REE to fit Eq. (33) yielding, with a standard deviation of 3887 J, the following:

$$RT\ln\left(\frac{D_o^{3+} \cdot X^{M1}_{Mg}}{Mg\#_{melt}}\right) - 7050P + 770P^2 = 88750 - 65.644T \tag{34}$$

Again the results are thermodynamically reasonable. The estimated entropy of fusion ($65.64\,J\,mol^{-1}\,K^{-1}$) is virtually identical to that of jadeite and the volume of fusion is about half that of the hypothetical $Na_{0.5}REE_{0.5}MgSi_2O_6$ pyroxene and one third that of jadeite. This suggests that most of the volume of fusion

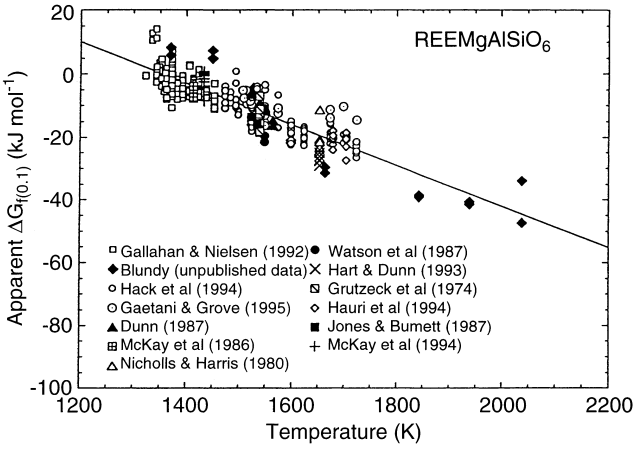

Fig. 10 The apparent 0.1 MPa free energy of fusion of hypothetical $REEMgAlSiO_6$ pyroxene plotted as a function of temperature. Available experimental data for all REE and Y are plotted. Again the strain energy of REE substitution was removed using Eq. (10)

of $Na_{0.5}REE_{0.5}MgSi_2O_6$ is due to the Na-component. The fictive 0.1 MPa temperatures of fusion of the end-members are also in reasonable progression: 943 K for jadeite (Blundy et al. 1995), 1260 K for $Na_{0.5}REE_{0.5}MgSi_2O_6$, and 1352 K for $REEMgAlSiO_6$.

Figure 10 shows the left hand side of Eq. (34) evaluated for all 481 points, plotted against temperature. As can be seen, the scatter is slightly worse than for the $Na_{0.5}REE_{0.5}MgSi_2O_6$ component, but the temperature dependence is clear and, as suggested above, thermodynamically reasonable. Furthermore, the simple activity-composition relations appear to remove any observable melt-compositional dependence of partition coefficient. Turning to the apparent standard deviation of 3887 J, one important contribution comes from the 27 unpublished points obtained on the join diopside-albite in our laboratory. We included them because they provide constraints on the fit equation at pressures up to 6 GPa and at temperatures up to 2038 K. Several of the bulk liquid compositions are extremely sodic, however, containing up to 60 mol% $NaAlSi_2O_6$ component and they show more scatter around the best-fit line than do most of the other data on more normal basaltic compositions. If we exclude these unpublished data from the estimate then the remaining 454 points fit Eq. (34) with a standard error of 3543 J. Of this uncertainty, we have already shown that 2762 J accrues from the uncertainty in the strain-radius correction. Using normal error propagation this means that the errors introduced by the thermodynamic approximations are $\sqrt{(3542^2 - 2762^2)}$ or 2217 J. This corresponds to a 1σ error in calculated partition coefficient, arising from the thermodynamic models, of 19%, a value smaller than that arising from the uncertainty in radius-strain correction. It should be noted that this relatively small scatter arises from a very wide range of bulk liquid compositions. The 454 points encompass anhydrous liquids with between 38 and 60 weight% SiO_2, 2–20% MgO, 0–22% FeO, 0–5% Na_2O and 0–3% K_2O. We conclude that the simple thermodynamic models may be joined to the strain energy equations to produce an Eq. (34) capable of calculating REE clinopyroxene-liquid partition coefficients with an uncertainty comparable to that involved in measuring them experimentally.

Practical application to D_{REE}

Having obtained a good description of partition coefficient as a function of bulk composition, pressure and temperature, we now consider how the results may best be applied to petrological problems. Potential applications are very widespread and include the precise quantification of D_{REE} during polybaric fractional melting of the mantle, reconstruction of liquid REE compositions from cumulus and intercumulus clinopyroxene in layered intrusions, and quantification of fractional crystallisation paths in systems crystallising clinopyroxene. The unsatisfactory conventional practice of adopting constant-value clinopyroxene-melt partition coefficients from the literature when tackling complex polybaric, polythermal petrological problems involving clinopyroxene can now be discontinued. For a given petrological problem the accuracy of a calculated partition coefficient depends on the nature of the available data. We will consider each of the possible scenarios in turn. In each case we will assume that pressure and temperature are approximately known.

a) Crystal bulk composition and one REE partition coefficient known

This is the simplest and most accurate situation

1. Use Eq. (15) to calculate r_o from the crystal composition.
2. Use Eq. (14) to calculate E^{3+}_{M2} at the pressure and temperature of interest.
3. Use D_i, the known REE partition coefficient, in conjunction with r_i, the ionic radius of this element, to calculate D^{3+}_o from Eq. (10).
4. With the values of D^{3+}_o, E^{3+}_{M2} and r_o the value of D_i for any REE of radius r_i is calculated from Eq. (10).

This method has, as shown in Fig. 6, a greater than 90% probability of being within 0.73 times and 1.36 times the true value.

b) Crystal and liquid bulk compositions known: no REE partitioning data available

Repeat steps (1) and (2) as before.

3. Use the bulk compositions to calculate $Mg\#_{melt}$ and X^{M1}_{Mg} in the clinopyroxene using the method of Wood and Banno (1973), i.e. Fe and Mg are partitioned equally between M1 and M2 sites.

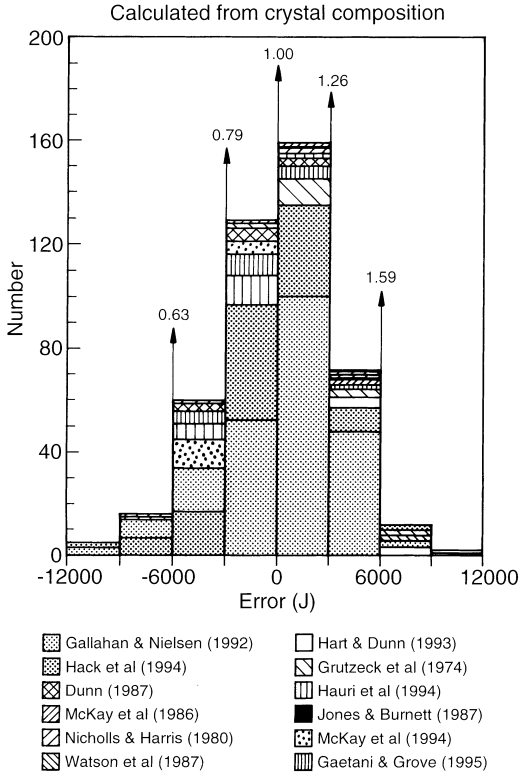

Fig. 11 Histogram of 454 points showing the error in $RT \ln D_{REE}$ which arises when D_o^{3+} is obtained from the thermodynamic model of Eq. (34), and Eqs. (10), (14) and (15) are used to calculate the values of D_{REE} under the same conditions. More than 92% of calculated D_{REE} values are within 0.63 and 1.59 times those experimentally observed, as shown by the *numbered arrows*

4. Calculate D_o^{3+} from Eq. (34).

5. With the values of D_o^{3+}, E_{M2}^{3+} and r_o the value of D_i for any REE of radius r_i is calculated from Eq. (10).

As shown in Fig. 11 this method gives D_{REE} with $> 92\%$ probability of being within 0.63 and 1.59 of the true value.

c) Crystal composition only available

Repeat steps (1) and (2) as before.

3. Calculate X_{Mg}^{M1} for the clinopyroxene as in b) above.

4. a *If* coexisting olivine is present then $Mg\#_{melt}$ can be predicted quite accurately from the forsterite content of the olivine, X_{Fo}:

$$Mg\#_{melt} = \frac{K_{Fe-Mg}^{ol} X_{Fo}}{1 - X_{Fo} + X_{Fo} K_{Fe-Mg}^{ol}}$$

where K_{Fe-Mg}^{ol} is the ratio of Fe/Mg in olivine to that in the melt. Experimentally measured values of K_{Fe-Mg}^{ol} are in the range 0.27–0.33 for most values of X_{Mg}^{ol} and the error associated with the adoption of a value of 0.30 (Roeder and Emslie 1970) is only 5–10% for most bulk compositions. This error translates directly into the same percentage error in D_{REE}.

Or

4. b *If* there is no coexisting olivine then the pyroxene composition must be used to estimate $Mg\#_{melt}$. This is more difficult because of the wide range of M2 contents of Fe and Mg which are present in natural clinopyroxenes. From the experimental data used in this study we find correlations between K_{Fe-Mg}^{cpx} and either temperature or X_{Mg}^{cpx}. We used the latter to derive the following expression:

$$K_{Fe-Mg}^{cpx} = 0.109 + 0.186\ Mg\#_{cpx} \tag{35}$$

where $Mg\#_{cpx}$ is the molar ratio of Mg to $Mg + Fe_{total}$ in the clinopyroxene. The clinopyroxene composition is therefore used to calculate K_{Fe-Mg}^{cpx} from (35) then, as in 4.a, the $Mg\#_{melt}$ is obtained as follows:

$$Mg\#_{melt} = \frac{K_{Fe-Mg}^{cpx} Mg\#_{cpx}}{1 - Mg\#_{cpx} + Mg\#_{cpx} K_{Fe-Mg}^{cpx}}$$

We find that this equation predicts the $Mg\#_{melt}$ to within 18% in 90% of the 211 experiments used here.

5. Calculate D_o^{3+} from Eq. (34)

6. With the values of D_o^{3+}, E_{M2}^{3+} and r_o the value of D_i for any REE of radius r_i is calculated from Eq. (10).

d) Melt composition only known

This is the most difficult and probably the most common application. We approach this by using the liquid composition to calculate the composition of the coexisting pyroxene at the pressure and temperature of interest. This procedure is detailed in the Appendix.

Despite the requirement to calculate the bulk composition of the pyroxene in order to determine r_o and X_{Mg}^{M1}, this approach, calculating directly from liquid composition, produces surprisingly good results. Comparing calculated D_{REE} with measured values we obtain a standard deviation of 3910 J (Fig. 12). Therefore in over 90% of cases, calculated D is in the range 0.60–1.67 of the true D, a scatter which is only about 8% worse than in the case where the pyroxene composition is actually known.

Concluding remarks

We have shown that the partition coefficients of REE and Y between clinopyroxene and liquid depend, as predicted from the Brice (1975) model, on the ionic radius of the cation, on the radius of the pyroxene M2 site into which they substitute, and on the apparent Young's modulus of the site. Using experimentally determined REE partition coefficients obtained over wide ranges of pressure (0.0001–6 GPa), temperature (1323–2038 K) and bulk composition we have shown the following:

1. The apparent Young's modulus of the M2 site depends, in agreement with the suggestion of Blundy and Wood (1994), approximately linearly on the charge on the cation such that:

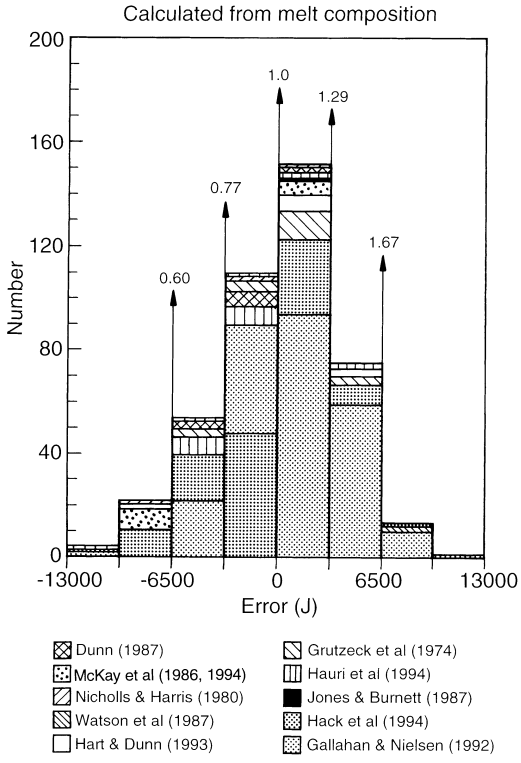

Fig. 12 Histogram of 454 points showing the error in $RT \ln D_{\mathrm{REE}}$ which arises when the major element composition of the clinopyroxene is calculated from the melt composition (see Appendix). D_o^{3+} is then obtained from Eq. (34), and Eqs. (10), (14) and (15) are used to calculate the values of D_{REE} under the same conditions. More than 90% of calculated D_{REE} values are within 0.60 and 1.67 times those experimentally observed, as shown by the *numbered arrows*

$$E_{\mathrm{M2}}^{1+} \approx \tfrac{1}{2} E_{\mathrm{M2}}^{2+} \approx \tfrac{1}{3} E_{\mathrm{M2}}^{3+}$$

Furthermore, the apparent Young's modulus for 2+ ions substituting into M2, E_{M2}^{2+}, is similar to the value for bulk diopside, indicating that the properties of the large M2 site control the bulk elastic properties of the crystal. This observation can be used to make approximations regarding the temperature and pressure sensitivity of E_{M2}^{3+}:

$$E_{\mathrm{M2}}^{3+} \approx 1.5 E_{\mathrm{diopside}} = 318.6 + 6.9P - 0.036T \qquad \text{GPa}$$

2. The radius of the clinopyroxene M2 site depends primarily on its Ca content and on the Al content of M1:

$$r_o = 0.974 + 0.067 X_{\mathrm{Ca}}^{\mathrm{M2}} - 0.051 X_{\mathrm{Al}}^{\mathrm{M1}} \text{ Å}$$

No other physical or chemical variables (including pressure) were found to be significant. The total range in r_o is 0.979–1.055Å (i.e. r_{Lu}–r_{Gd}), with an uncertainty of ±0.009Å. The clinopyroxenes contain between 0 and 21% $NaAlSi_2O_6$ component and have *Mg* numbers between 0.63 and 1.0.

3. Given the partition coefficient of a middle REE such as Sm or Gd the values of *D* for all the other REE can be predicted accurately using the Brice Eq. (10) with uncertainties which are approximately the same as those involved in measuring *D*. In practice 92% of 251 values could be predicted to within 0.73–1.36 times the independent measurement.

4. Partitioning of the "ideal" REE (i.e. radius r_o) can be described thermodynamically in terms of equilibria involving either of the coupled substitutions $\mathrm{Na} + \mathrm{REE} \Leftrightarrow 2\mathrm{Ca}$ or $\mathrm{REE} + \mathrm{Al} \Leftrightarrow \mathrm{Ca} + \mathrm{Si}$. A simple thermodynamic model for the melt in which 6-oxygen units such as $CaMgSi_2O_6$, $NaAlSi_2O_6$ and $REEMgAlSiO_6$ are assumed to mix ideally works well for anhydrous silicate melts over a wide range of composition. In practice we find that the ideal partition coefficient D_o for element of radius r_o may be calculated from:

$$RT \ln\left(\frac{D_o^{3+} \cdot X_{\mathrm{Mg}}^{\mathrm{M1}}}{Mg\#_{\mathrm{melt}}}\right) - 7050P + 770P^2 = 88750 - 65.644T$$

Combining this equation and the Brice Eq. (10) we find that > 92% of REE partition coefficients can be calculated to within 0.63–1.59 times the measured value.

5. Clinopyroxene bulk composition can also be calculated from the melt composition with sufficient accuracy for r_o to be estimated from Eq. (15). Only a small additional uncertainty arises in predicted D_{REE}, relative to the case in which both clinopyroxene and melt compositions are known.

We consider that the dependencies of clinopyroxene rare earth element partition coefficients on pressure, temperature and bulk composition in anhydrous silicate melts are now sufficiently well known for the collection of experimental data on specific natural bulk compositions to be unnecessary. Experimental work now needs to be focused on understanding the details of melt-compositional effects which our simple melt model has lost in the scatter of the partition coefficient data. In particular we require information on the effect of dissolved water on the partitioning of REE and other cations. At present the expressions introduced here remain untested on hydrous systems.

Our model can be applied to a wide range of geochemical problems involving clinopyroxene. Not only does the model enable the appropriate D_{REE} to be calculated for the pressure, temperature, composition conditions of interest, but for polybaric, polythermal processes variations in D_{REE} in response to changing pressure and temperature can be quantitatively incorporated into models. Specific applications include: adiabatic decompression melting of the mantle, wherein at pressures less than ~ 2.5 GPa clinopyroxene is the principal host for the REE; calculation of melt REE composition from clinopyroxene composition in cumulates or other plutonic rocks where melts are not preserved; prediction of the behaviour in magmatic systems of trace cations that are not amenable to experimental study, e.g. trivalent actinides. The approach is based on a simple causative link between mineral physics and trace element geochemistry, and is therefore readily generalisable to other mineral-melt systems.

Acknowledgements B.J.W. acknowledges the support of the Alexander von Humboldt Stiftung at the Mineralogisches Institut,

Universität Freiburg where most of this work was done. J.D.B. wishes to thank NERC and the Royal Society for research fellowships. A.W. Hofmann, C.J. Allègre, W. van Westrenen and an anonymous reviewer provided informed comments on the manuscript and its unashamedly determinist philosophy.

Appendix: calculation of clinopyroxene composition and D_{REE} from melt composition

The methodology uses the liquid-solid partitioning of $NaAlSi_2O_6$ and $CaMgSi_2O_6$ components discussed above, to estimate the Ca and Na occupancies of the M2 site. Additional data required are $Mg\#$, Ti, Cr and $CaAl_2SiO_6$ contents of the pyroxene. Empirical equations for these were obtained from observed liquid-solid partitioning in the experiments discussed here and those of Falloon and Green (1987), Kinzler and Grove (1992) and Blundy et al. (1995; appendix). The method operates at fixed pressure and iterates temperature, from an initial estimate, until the liquid reaches clinopyroxene saturation, which is taken to be the point at which the Ca + Na content of the M2 site falls within a predetermined range. It works as follows:

1. Read in melt composition in weight% oxides (SiO_2, TiO_2, Al_2O_3, Cr_2O_3, FeO, MnO, MgO, CaO, Na_2O, K_2O); generally all Fe has been taken as FeO
2. Read in pressure (GPa) and an initial estimate of temperature (K)
3. Convert melt composition to moles
4. Calculate amounts of each cation (Si, Ti, Al, Cr, Fe, Mn, Mg, Ca, Na, K) to a total of 6 oxygens in the melt
5. Recalculate cations to 6-oxygen "molecules" as follows:

$$\mathrm{Na} = \mathrm{NaAlSi_2O_6}\ (JD)$$

$$\mathrm{K} = \mathrm{KAlSi_2O_6}\ (KT)$$

$$\mathrm{Ti} = \mathrm{CaTiAl_2O_6}\ (CT)$$

$$(\mathrm{Al} - 2\mathrm{Ti} - \mathrm{Na} - \mathrm{K}) = \mathrm{CaAl_2SiO_6}(CATS)$$

$$\mathrm{Ca} - \mathrm{CaAl_2SiO_6} - \mathrm{CT} = \mathrm{Ca(Mg,Fe,Mn)Si_2O_6}\ (DI)$$

$$\tfrac{1}{3}[\mathrm{Mg} + \mathrm{Fe} + \mathrm{Mn} - \mathrm{Ca(Mg,Fe,Mn)Si_2O_6}] = \mathrm{(Mg,Fe,Mn)_3Si_{1.5}O_6}\ (OL)$$

$$\tfrac{1}{3}[\mathrm{Si} - 2\mathrm{K} - 2\mathrm{Na} - 2\mathrm{Ca(Mg,Fe,Mn)Si_2O_6} - \mathrm{CaAl_2SiO_6} - 1.5\mathrm{(Mg,Fe,Mn)_3Si_{1.5}O_6}] = \mathrm{Si_3O_6}\ (QZ)$$

6. Calculate the mole fraction of $NaAlSi_2O_6$, X_{jd}^{cpx}, in the crystal from the expression of Blundy et al. (1995) using the jadeite content of the liquid (JD) at fixed P (GPa) and T(K):

$$X_{jd}^{cpx} = JD \times \exp\left(\left(\frac{10367 + 2100P - 165P^2}{T}\right) \cdot \left(-10.27 + 0.358P - 0.0184P^2\right)\right)$$

7. Calculate Ti content of clinopyroxene M1 site X_{Ti}^{cpx} using approximate relationship between CT in the liquid and X_{jd}^{cpx}:

$$X_{Ti}^{cpx} = CT \times \left(0.374 + 1.5X_{jd}^{cpx}\right)$$

8. Use similar empirical partitioning data to calculate Cr in crystal M1 site X_{Cr}^{cpx} from moles of Cr in melt per 6 oxygens

$$X_{Cr}^{cpx} = 5\mathrm{Cr}$$

9. Calculate the $Mg\#_{cpx}$ from $Mg\#_{melt}$ (if there is no Fe in the system, set both values to 1.0 and by-pass this calculation)

$$A = \frac{Mg\#_{melt}}{(1 - Mg\#_{melt})}$$

$$B = 0.108 + 0.323Mg\#_{melt}$$

$$Mg\#_{cpx} = \frac{A}{A + B}$$

10. Calculate the activity of $CaAl_2SiO_6$ component in the clinopyroxene (a_{CaTs}^{cpx}), from the product of Ca per 6 oxygens in the liquid and Al per 6 oxygens (less the Al in $CaTiAl_2O_6$):

$$a_{CaTs}^{cpx} = (CT + CATS + DI) \times (CATS + JD + KT) \times \exp\left(\frac{76469 - 62.078T + 12430P - 870P^2}{8.314T}\right)$$

Apply an upper limit to ensure pyroxene is not unreasonably aluminous:

IF $(a_{cats}^{cpx} > 0.4)$ THEN $a_{cats}^{cpx} = 0.4$

11. Similar approach to calculate activity of $CaMgSi_2O_6 (a_{Di}^{cpx})$ from the (DI) content of the liquid using a parabolic pressure dependence of volume instead of a full Birch-Murnaghan treatment:

$$a_{di}^{cpx} = DI \times Mg\#_{melt} \exp\left(\frac{132650 - 82.152T + 13860P - 1130P^2}{8.314T}\right)$$

12. Use calculated a_{CaTs}^{cpx} and a_{Di}^{cpx} to calculate X_{Ca}^{M2}, the Ca content of the M2 site:

$$X_{Ca}^{M2} = \frac{a_{CaTs}^{cpx} Mg\#_{cpx} + a_{Di}^{cpx}}{Mg\#_{cpx}(1 - X_{Cr}^{cpx} - X_{Ti}^{cpx})}$$

13. Check for clinopyroxene saturation by calculating whether Ca plus Na in M2 lies within the predetermined range, if not then modify temperature estimate

$$\mathrm{SUM} = X_{Ca}^{M2} + X_{jd}^{cpx}$$

$$\mathrm{TEST} = 0.92\text{–}0.55(1 - Mg\#_{cpx})$$

IF(SUM > TEST) **THEN** $T = T + 20$

RETURN to step (6)

$$\mathrm{TEST2} = 0.85\text{–}1.1\ (1 - Mg\#_{cpx})$$

IF(SUM < TEST2) **THEN** $T = T - 14$

RETURN to step (6)

14. Calculate the size of the M2 site

$$r_o = 0.974 + 0.067X_{Ca}^{M2} - 0.051\left(\frac{a_{CaTs}^{cpx}}{X_{Ca}^{M2}}\right)$$

15. Calculate the equilibrium constant (K_{REE}) for the reaction involving $REEMgAlSiO_6$ component. (Note that the thermodynamic properties are very slightly different from the quoted values which started from solid composition because we found a small average offset of 241 J when starting from the liquid composition)

$$K_{REE} = \exp\left(\frac{-88509 + 65.664T - 7050P + 770P^2}{8.314T}\right)$$

16. Calculate D_o^{3+} from the equilibrium constant using crystal and liquid compositions

$$X_{Mg}^{M1} = Mg\#_{cpx}\left(1 - X_{Cr}^{cpx} - X_{Ti}^{cpx} - \left(\frac{a_{cats}^{cpx}}{X_{Ca}^{M2}}\right)\right)$$

$$D_o^{3+} = \frac{Mg\#_{melt}}{K_{REE} \cdot X_{Mg}^{M1}}$$

17. Use Eq. (14) to calculate E_{M2}^{3+} at the pressure and temperature of interest
18. With the values of D_o^{3+}, E_{M2}^{3+} and r_o the value of D_i for any REE of radius r_i is calculated from Eq. (10)

References

Anderson DL (1989) Theory of the Earth. Blackwell Scientific, Oxford

Anderson DL, Anderson OL (1970) The bulk modulus-volume relationship for oxides. J Geophys Res 75: 3494–3500

Beattie P (1994) Systematics and energetics of trace-element partitioning between olivine and silicate melts: implications for the nature of mineral/melt partitioning. Chem Geol 117: 57–71

Blundy JD, Wood BJ (1991) Crystal-chemical controls on the partitioning of Sr and Ba between plagioclase feldspar, silicate melts and hydrothermal solutions. Geochim Cosmochim Acta 55: 193–209

Blundy JD, Wood BJ (1994) Prediction of crystal-melt partition coefficients from elastic moduli. Nature 372: 452–454

Blundy JD, Falloon TJ, Wood BJ, Dalton JA (1995) Sodium partitioning between clinopyroxene and silicate melts. J Geophys Res 100: 15501–15516

Blundy JD, Wood BJ, Davies A (1996) Thermodynamics of trace element partitioning between clinopyroxene and melt in the system CaO-MgO-Al_2O_3-SiO_2. Geochim Cosmochim Acta 60: 359–364

Brice JC (1975) Some thermodynamic aspects of the growth of strained crystals. J Cryst Growth 28: 249–253

Burnham CW (1981) The nature of multicomponent aluminosilicate melts. Phys Chem Earth 13: 197–229

Drake MJ (1972) The distribution of major and trace elements between plagioclase feldspar and magmatic silicate liquid: an experimental study (unpublished). PhD thesis, Univ Oregon, Eugene, Oregon, USA

Dunn T (1987) Partitioning of Hf, Lu, Ti and Mn between olivine, clinopyroxene and basaltic liquid. Contrib Mineral Petrol 96: 476–484

Falloon TJ, Green DH (1987) Anhydrous partial melting of MORB pyrolite and other peridotite compositions at 10 kbar: implications for the origin of primitive MORB glasses. Mineral Petrol 37: 181–219

Finger LW, Ohashi Y (1976) The thermal expansion of diopside to 800 °C and a refinement of the crystal structure at 700 °C. Am Mineral 61: 303–310

Gaetani GA, Grove TL (1995) Partitioning of rare earth elements between clinopyroxene and silicate melt: crystal-chemical controls. Geochim Cosmochim Acta 59: 1951–1962

Gallahan WE, Nielsen RL (1992) The partitioning of Sc, Y and the rare earth elements between high-Ca pyroxene and natural mafic to intermediate lavas at 1 atmosphere. Geochim Cosmochim Acta 56: 2387–2404

Grutzeck M, Kridelbaugh S, Weill D (1974) The distribution of Sr and REE between diopside and silicate liquid. Geophys Res Lett 1: 273–275

Hack PJ, Nielsen RL, Johnston AD (1994) Experimentally determined rare-earth element and Y partitioning behaviour between clinopyroxene and basaltic liquids at pressures up to 20 kbar. Chem Geol 117: 89–105

Hart SR, Dunn T (1993) Experimental cpx/melt partitioning of 24 trace elements. Contrib Mineral Petrol 113: 1–8

Hauri EH, Wagner TP, Grove TL (1994) Experimental and natural partitioning of Th, U, Pb and other trace elements between garnet, clinopyroxene and basaltic melts. Chem Geol 117: 149–166

Hazen RM, Finger LW (1979) Bulk modulus-volume relationship for cation-anion polyhedra. J Geophys Res 84: 6723–6728

Holland TJB (1990) Activities of components in omphacite solid solutions. Contrib Mineral Petrol 105: 446–553

Jones JH (1995) Experimental trace element partitioning. In: Ahrens TJ (ed) Rock physics and phase relations: a handbook of physical constants. Am Geophys Union Reference Shelf 3: 73–104

Jones JH, Burnett DS (1987) Experimental geochemistry of Pu and Sm and the thermodynamics of trace element partitioning. Geochim Cosmochim Acta 51: 769–782

Kinzler RJ, Grove TL (1992) Primary magmas and mid-ocean ridge basalts. 1. Experiments and methods. J Geophys Res 97: 6885–6906

Lagache M, Dujon SC (1987) Distribution of strontium between plagioclases and 1 molar aqueous chloride solutions at 600 °C, 1.5 kbar and 750 °C, 2 kbar. Bull Mineral 110: 551–561

Lange RA, Carmichael ISE (1990) Thermodynamic properties of silicate liquids with emphasis on density, thermal expansion and compressibility. Rev Mineral 24: 25–64

Litvin YA, Gasparik T (1993) Melting of jadeite to 16.5 GPa and melting relations on the enstatite-jadeite join. Geochim Cosmochim Acta 57: 2033–2040

Liu C-Q, Masuda A, Shimizu H, Takahashi K, Xie G-H (1992) Evidence for pressure dependence of the peak position in the REE mineral/melt partition patterns of clinopyroxene. Geochim Cosmochim Acta 56: 1523–1530

McKay GA, Wagstaff J, Yang SR (1986) Clinopyroxene REE distribution coefficients for shergottites: the REE content of the Shergotty melt. Geochim Cosmochim Acta 50: 927–937

McKay G, Le L, Wagstaff J, Crozaz G (1994) Experimental partitioning of rare earth elements and strontium: constraints on the petrogenesis and redox conditions during crystallisation of Antarctic angrite Lewis Cliff 86010. Geochim Cosmochim Acta 58: 2911–2919

Mysen BO (1990) Relationships between silicate melt structure and petrologic processes. Earth-Sci Rev 27: 281–365

Nagasawa H (1966) Trace element partition coefficient in ionic crystals. Science 152: 767–769

Nicholls IA, Harris KL (1980) Experimental rare earth element partition coefficients for garnet, clinopyroxene and amphibole coexisting with andesitic and basaltic liquids. Geochim Cosmochim Acta 34: 331–340

Nielsen RL (1988) A model for the simulation of the combined major and trace element liquid lines of descent. Geochim Cosmochim Acta 52: 27–38

Press WH, Flannery BP, Teukolsky SA, Vetterling WT (1986) Numerical recipes. Cambridge Univ Press, Cambridge

Richet P, Bottinga Y (1986) Thermochemical properties of silicate liquids and glasses: a review. Rev Geophys 24: 1–25

Robie RA, Hemingway BS, Fisher JR (1979) Thermodynamic properties of minerals and related substances at 298.15 K and 1 bar (10^5) pascals. US Geol Surv Bull 1452

Roeder PL, Emslie RF (1970) Olivine-liquid equilibrium. Contrib Mineral Petrol 21: 275–289

Shannon RD (1976) Revised effective ionic radii in oxides and fluorides. Acta Crystallogr A32: 751–757

Shaw DM (1970) Trace element fractionation during anatexis. Geochim Cosmochim Acta 34: 237–243

Smyth JR, Bish DL (1988) Crystal structures and cation sites of the rock forming minerals. Allen and Unwin, Boston

Sumino Y, Anderson OL (1984) Elastic constants of minerals. In: Carmichael RS (ed) Handbook of physical properties of rocks. CRC Press, Boca Raton, FL, pp 39–138

Takahashi E (1986) Melting of a dry peridotite KLB-1 up to 14 GPa: implications on the origin of peridotitic upper mantle. J. Geophys Res 91: 9367–9382

Walter MJ, Presnall D (1994) Melting behaviour of simplified lherzolite in the system CaO-MgO-Al_2O_3-SiO_2-Na_2O from 7 to 35 kbar. J Petrol 35: 329–359

Watson EB, Ben Othman D, Luck JM, Hofmann AW (1987) Partitioning of U, Pb, Cs, Yb, Hf, Re and Os between chromian diopsidic pyroxene and haplobasaltic liquid. Chem Geol 62: 191–208

Williams DW, Kennedy GC (1969) The melting curve of diopside to 50 kilobars. J Geophys Res 74: 4359–5366

Wood BJ (1987) Thermodynamics of multicomponent systems containing several solid solutions. Rev Mineral 17: 71–96

Wood BJ, Banno S (1973) Garnet-orthopyroxene and orthopyroxene-clinopyroxene relationships in simple and complex systems. Contrib Mineral Petrol 42: 109–124

Wood BJ, Fraser DG (1976) Elementary thermodynamics for geologists. Oxford Univ Press, Oxford